Z. Ladin

K. R. Murthy

C. J. De Luca

Biomedical Engineering Department and
NeuroMuscular Research Center,
Boston University
Boston, MA 02215

The Effects of External Bending Moments on Lumbar Muscle Force Distribution

A detailed biomechanical model of the low-back musculature that predicts muscle-force distribution in response to external loading is presented. The paper shows that the class of loading tasks that involve an erect posture and an arbitrary load placed on the upper limbs can be described as a loading plane whose axes are the flexion and lateral bending moments. Under these conditions, the individual muscle forces are described as a three-dimensional surface defined by the loading plane and termed the muscle activity surface (MAS). The MAS and the loading plane intersect along the switching curve which separates the load combinations that activate the muscle from those that do not. The paper suggests the existence of a recruitment order of low back muscles in response to external loads and presents a comprehensive framework for examining earlier studies that used EMG measurements to validate physiological and mechanical predictions.

Introduction

The role of the lumbar muscles in maintaining posture and balancing externally applied loads has been studied for many years. Preliminary studies (Golding 1952, Morris et al., 1962, Jonsson, 1970) used electromyography (EMG) to establish a relationship between trunk posture and muscle activity, thereby developing a better understanding of the functional role of those muscles. More recently, biomechanical models of the lower back have been developed to study the effect of loading tasks on the musculoskeletal system. Freivalds et al., (1984) and Kromodihardjo and Mital, (1987) analyzed the dynamics of lifting tasks and their effects on the loading of the spinal column. To avoid the added complexity that arises from variations in muscle length induced by postural changes, muscle force distribution studies have been limited to isometric contractions (Andersson et al., 1980; Schultz, et al., 1982, 1983; Seroussi and Pope, 1987, Bean et al., 1988). The main mode of testing muscle force predictions has been electromyographic studies by surface electrodes, and the comparison of the EMG amplitude to the predicted muscle force value (Schultz et al., 1983; Pope et al., 1986; Seroussi and Pope, 1987). Those studies found acceptable correlations between some muscle force predictions and muscular activity as measured by the EMG amplitude, but did not provide a comprehensive framework for studying the role of the different muscle groups in opposing external loads. This paper describes a new method for studying the role of individual muscles and predicted activation patterns used by the low-back muscles to oppose external loads. The method introduces the concept of muscle activity surfaces

(MASs), which are three-dimensional surfaces describing the individual muscle forces due to an external combination of bending moments: the lateral bending moment and the flexion-extension moment. The MAS intersects the loading plane (the plane defined by the the two bending moments) along a curve that is the muscle's *switching curve*. The muscle is predicted to be active on one side of this curve and inactive on the other side.

Methodology

Many joints in the human body behave as dynamic systems where the number of muscles crossing a joint exceeds the number of degrees of freedom (DOF) of that joint. Such joints are termed mechanically redundant systems, since in trying to solve for the individual muscle forces, one is faced with a number of unknowns (muscle forces) that exceeds the number of dynamic equations (that is equal to the number of DOF). As Crowninshield (1978) points out, two basic approaches have been used to address the mechanical redundancy: functional reduction and optimization. The first approach involves the use of anatomical or physiological assumptions to reduce the number of unknown muscle forces by grouping together different muscles, until the number of unknowns matches the number of DOF, thus making the problem determinate. The second approach uses an optimization technique and distributes the muscle forces such that a given criterion (a cost function) is optimized. Optimization approaches have been used to study the upper limb (Crowninshield, 1978), the lower limb (Crowninshield et al., 1978; Crowninshield and Brand, 1981; Patriarco et al., 1981, and the back (Schultz et al., 1983; Gracovetsky, 1986).

The study of muscle force distribution in the lower back

begins by performing a transverse cross-section at the level of interest (L_3 in our case) and conducting a "free body" analysis. This step results in six equilibrium constraint equations for the twenty-two unknown muscle forces, producing a highly redundant system. In writing the equilibrium equations we applied the physiological decoupling assumption introduced by Andersson et al. (1980), who suggested that the muscles crossing the lumbar region balanced the external moments, while the spinal reaction forces balanced the external forces and the resultant muscular forces. Hence, six equilibrium constraint equations (three force equations and three moment equations) were written for the individual unknown muscle tensile forces. The anatomical data is based on the original dissections of Eycleshymer and Schoemaker (1911) as approximated by Schultz et al. (1983). It includes twenty-two muscles that cross the L_3 level of the lumbar region, where each muscle is approximated as a circle whose center and area correspond to the values obtained in the original dissection.

The optimization scheme used in this study consists of the definition and minimization of a cost function subject to the moment equilibrium constraints and muscle stress inequality constraints. While there are a number of cost functions that can be utilized, Schultz et al. (1983) reported that the scheme that produced the best correlations between predicted muscle forces and the measured EMG signals used the minimization of the spinal compression while placing an upper boundary on the muscle stresses. A modified version of this scheme, which defined the cost function as the spinal compression due only to the muscle forces was employed in this model. This cost function is termed in this paper the muscular spinal compression function. The muscle stress inequality constraints required the individual stresses to be positive and not to exceed a given maximum stress level. The appendix gives a detailed description of the mathematical formulation of the model. The physical tasks analyzed in this study involve gravitational loading on the upper extremity. Such tasks represent subjects standing erect and holding weights in arbitrarily positioned hands. The external moment loading on a transverse plane in the lumbar region is composed of two bending moments: M_x- the flexion-extension moment, and M_y the lateral bending moment. The external torsion torque and horizontal forces are all zero. Under these conditions the external loading is uniquely defined by the combination of the bending moments (M_x, M_y). Thus, a "loading plane" whose axes are M_x and M_y can be generated. This plane represents the possible loading combinations that arise from changing the hand-held load and/or the position of the upper limbs. By calculating the bending moments that result from a particular physical task a mapping from the task to a single point on the loading plane can be obtained.[1]

A linear programming algorithm was used to scan the solution space (whose axes are the unknowns) to find a com-

bination of muscle forces that minimizes the cost function. The requirement that the muscle forces be positive and upper bounded (i.e., not exceeding a maximum value) narrows the search for a minimum to a bounded region of the solution space. The moment equality constraints, represented by linear equations, further limit the search to given combinations of the unknowns that satisfy these equations. Hence, either an optimal solution exists in the bounded region, or no solution exists and the upper bounds on the muscle forces have to be increased, and the search for the minimum must be repeated. The result is a set of muscle forces for a given combination of bending moments.

Since a single moment load combination (M_x, M_y) produces a single muscle force prediction, the individual muscle tension can now be described as a surface (termed the muscle activity surface-MAS) defined on the (M_x, M_y) plane. Such a surface fully characterizes the tension in a particular muscle due to arbitrary gravitational loadings. The process of generating the surface involves the following steps:

1. Select a combination of moments (M_x, M_y).
2. Minimize the muscular spinal compression cost function subject to the three moment equation constraints $(M_x, M_y,$ and $M_z)$ and inequality constraints.
3. Store the resulting muscle force distribution.
4. Change the (M_x, M_y) combination until the portion of the (M_x, M_y) plane that is of interest has been covered.

The model was implemented on a VAX 11/8520 computer, using optimization routines from the IMSL library. The iterative process involved the specification of a low stress level as the upper bound for the calculations of the individual muscle forces. If a solution could not be obtained, i.e., the muscle forces resulting from the given stress level were insufficient to balance the external loading moments, the upper bound was increased and the optimization routine was repeated until convergence (subject to the moment equality constraints) was achieved.

Results

The consistency of the model was tested by comparing the muscle force patterns produced by symmetric loading conditions. The individual forces were calculated for combinations of $(M_x; M_y)$ and $(M_x; -M_y)$ representing loading conditions of equal flexion moments and symmetric lateral bending moments. These patterns were found to be symmetric for the pairs of contralateral muscles: the muscle force in the right multifidus in response to a load combination (M_x, M_y) is equal to the muscle force in the left multifidus in response to a load combination $(M_x, -M_y)$ (see Table 1).

The distribution of the muscle forces and the corresponding muscle stresses for two different tasks are shown in Figs. 1 and 2. Figure 1(a) describes the muscle activity pattern produced by the task illustrated by the stick figure (the right upper limb is horizontally abducted $0°$, holding a 5 kgf load). The muscle force distribution shows the activation of the muscles on the left side of the body that oppose the external load. On the right side the only active muscle is the rectus abdominus

---

[1]Note that the reverse statement is not true, i.e., a single point in the (M_x, M_y) plane corresponds to multiple physical tasks that could produce such a combination of moments.
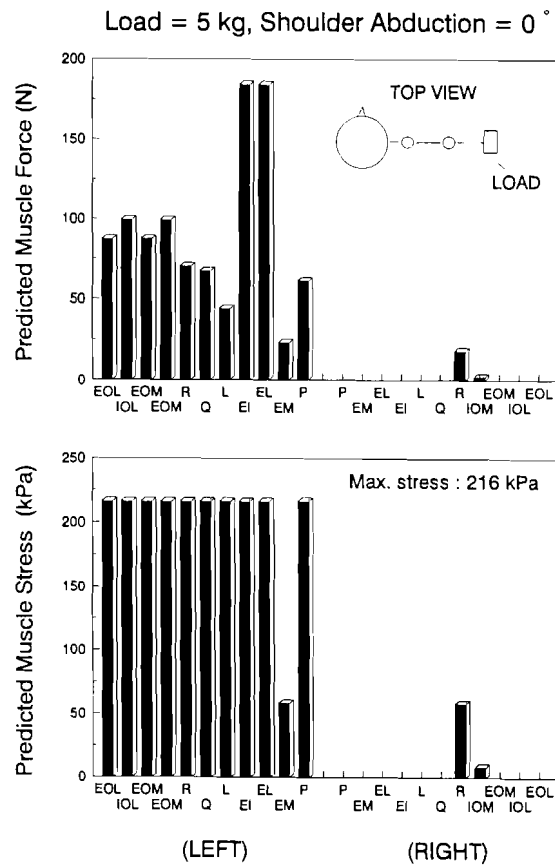

Nomenclature

M_x	=	flexion moment	P	=	Psoas muscle	
M_y	=	lateral bending moment	L	=	latissimus muscle	
EI	=	iliocostalis muscle	EOM	=	medial external oblique muscle	
EM	=	multifidus muscle				
EL	=	longissimus muscle	EOL	=	lateral external oblique muscle	
Q	=	quadratus Lumborum muscle				

IOM = medial internal oblique muscle
IOL = lateral internal oblique muscle
R = rectus abdominus muscle

Table 1 Muscle force in the right and left multifidus under different load combinations

Left Multifidus Muscle Force (N)

Flexion Moment (Nm)	\ Right Lateral Bending Moment (Nm) 0	10	20	30	40	50	60	70	80	90	100
0	0	6	24	41	59	77	94	112	118	136	153
10	20	27	37	50	65	80	95	110	125	140	155
20	40	44	53	64	75	88	101	115	130	144	159
30	61	63	70	80	90	100	112	125	138	151	165
40	81	84	88	97	107	117	127	138	150	163	178
50	101	104	107	113	123	133	144	154	164	176	187
60	121	124	127	132	140	150	160	170	181	191	201
70	142	144	147	150	157	166	176	186	197	207	217
80	162	165	167	170	175	183	193	203	213	223	234
90	182	185	188	190	194	201	210	220	230	240	250
100	202	205	208	210	213	220	226	236	246	256	266

Right Multifidus Muscle Force (N)

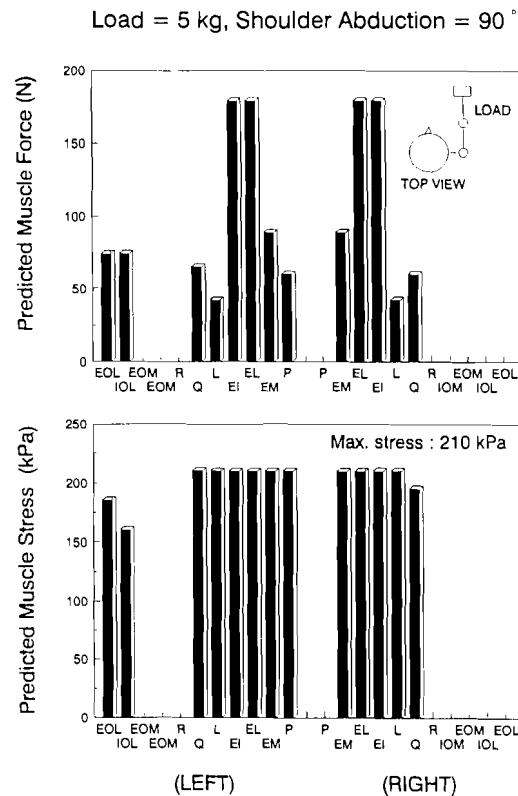| Flexion Moment (Nm)	\ Left Lateral Bending Moment (Nm) 0	10	20	30	40	50	60	70	80	90	100
0	0	6	24	41	59	77	94	112	118	136	153
10	20	27	37	50	65	80	95	110	125	140	155
20	40	44	53	64	75	88	101	115	130	144	159
30	61	63	70	80	90	100	112	125	138	151	165
40	81	84	88	97	107	117	127	138	150	163	178
50	101	104	107	113	123	133	144	154	164	176	187
60	121	124	127	132	140	150	160	170	181	191	201
70	142	144	147	150	157	166	176	186	197	207	217
80	162	165	167	170	175	183	193	203	213	223	234
90	182	185	188	190	194	201	210	220	230	240	250
100	202	205	208	210	213	220	226	236	246	256	266

Load = 5 kg, Shoulder Abduction = 0 °

Fig. 1 Muscle force (top) and stress (bottom) distributions in the lumbar region, due to a right lateral load of 5 kgf (0 deg abduction of the right shoulder)

(the medial portion of the internal oblique-IOM-provides an insignificant level of force). The longissimus (EL) and the iliocostalis (EI) are the muscles that bear the largest individual forces: their muscle force predictions are almost twice as large as the next muscle group (the internal oblique group of the abdominal muscles). Figure 1(b) describes the calculated muscle stresses that correspond to the force distribution pattern described in Fig. 1(a). There is a nearly uniform distribution of the individual muscle stresses on the left side. All the muscles on that side (with the exception of the multifidus) generate stresses of about 220 kPa.

Figure 2(a) shows the change in the muscle activity pattern resulting from a 90 deg horizontal abduction of the upper limb (from the posture indicated by Fig. 1). Hence, the right arm is now horizontally extended forward, holding the same load. The back muscles on the right side are much more active now, with five out of the six back muscles having equal force levels to the corresponding muscles on the left side. Three out of the five abdominal muscles on the left side have totally decreased their force output, with a similar decrease in the activity of the rectus abdominus on the right side.

Figure 2(b) describes the calculated muscle stresses that correspond to the same task. Again we can observe an almost uniform distribution with all the back muscles on both sides (with the exception of the right quadratus lumborum) of about 210 kPa. The active abdominal muscles on the left side have stress values that are 75–85 percent of the maximum muscular stress level above.

Figure 3 shows the activity surfaces of the bilateral iliocostalis muscles. The surface represents the muscle tension in the iliocostalis muscle for different values of external load (M_x, M_y). The perspective used in the figure masks the fact that the two

Load = 5 kg, Shoulder Abduction = 90 °

Fig. 2 Muscle force (top) and stress (bottom) distributions in the lumbar region due to a 5 kgf load held in the right hand in front of the body (90 deg abduction of the right shoulder).
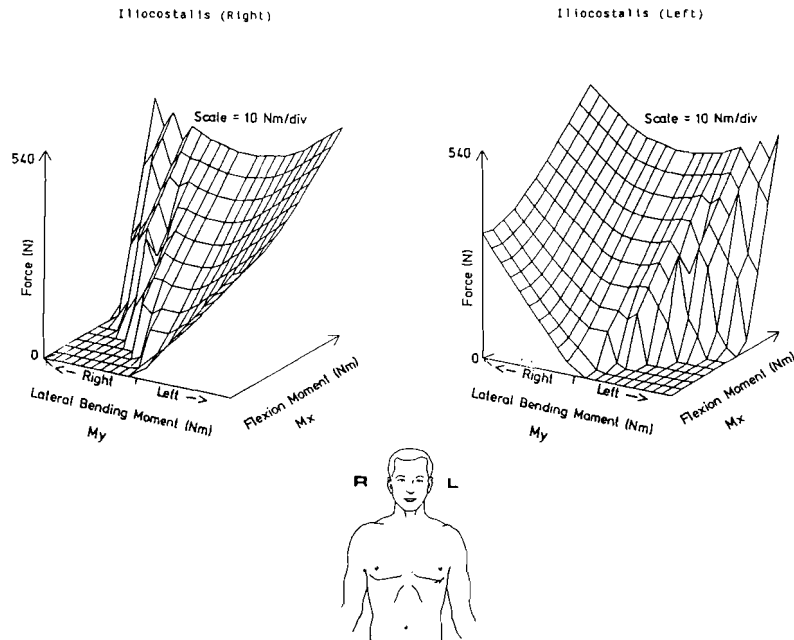
Fig. 3 Muscle activity surfaces of the right and left iliocostalis

surfaces are symmetric with respect to the $M_y = 0$ plane, i.e., the tension in the right muscle under the (M_x, M_y) load is equal to the tension in the left muscle under the $(M_x, -M_y)$ load; each surface by itself is not symmetric.

A close examination of each surface reveals some interesting properties of the dependence of the muscle tension on the external loading:

— there is a range of (M_x, M_y) values for which the muscle is inactive

— the surface intersects the (M_x, M_y) plane along a curve that is referred to as the *switching-curve*: (M_x, M_y) combinations on one side of the curve will not trigger any muscular activity, whereas values on the other side will activate the muscle (Fig. 4)

— the surface shows a *saddle* topology: a cross-section of the surface with a $M_x = $ constant plane shows a curve with a minimum at $M_y = 0$; intersecting the plane by a $M_y = $ constant plane shows a monotonically increasing curve

Figures 4 and 5 describe the activity surfaces of two additional back muscles on the left side: the longissimus (Fig. 4) and the multifidus (Fig. 5). These muscles' activity surfaces (Fig. 4-5) show the same saddle topology as the iliocostalis' activity surface (Fig. 3): a monotonically increasing surface with M_x, and a local minimum along the M_y axis. The surface increases monotonically for M_y that have large absolute values.

As defined above, the MAS intersects the loading plane along the switching-curve for that particular muscle. Since the surfaces of all the muscles are defined by the same plane, the switching curves of all the muscles are also defined by the same plane, and therefore they can be graphically overlaid as was done in Fig. 6. This figure describes the switching curves of five muscles on the left side of the body. They consist of two back muscles (the multifidus and the quadratus) and three abdominal muscles (the rectus abdominus, the medial portion of the internal obique and the lateral portion of the external oblique). As each curve divides the loading plane (M_x, M_y) into two regions-one where the muscle is inactive and the other where the muscle is active, it is possible to determine the muscles that will be active for a given load. For example: at point A, that represents a loading condition of a 10 Nm flexion

Longissimus (left)
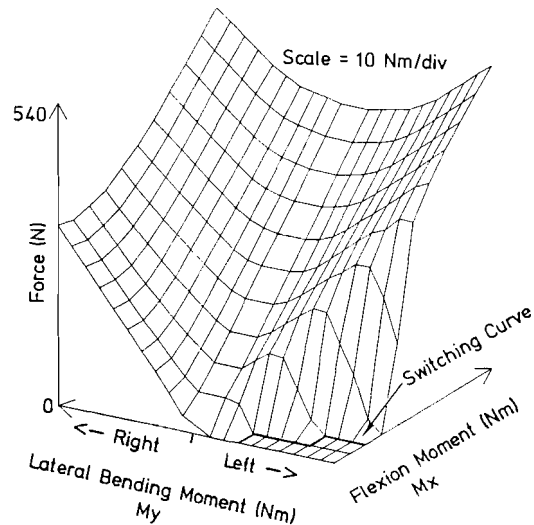
Fig. 4 Muscle activity surface of the left longissimus illustrating the switching curve for this muscle

moment and a 75 Nm left lateral bending moment, none of the above muscles are active; at point B, only the multifidus becomes active; at C, the quadratus joins in; at D, the external oblique is activated and joins the previously indicated muscles; at E, the internal oblique becomes active and at F, all the muscles are active. By selecting an appropriate set of weights, one can design an exercise that will generate the loading conditions described by the points A-F. Such an exercise will start by holding the weight in the left hand (negative M_y, small M_x), horizontally abducting the left upper limb (increasing both M_x and M_y), holding the load in front of the body in a symmetric fashion ($M_y = 0$), and then transferring the load to the right hand and horizontally abducting the right upper limb 90 degrees (thus reducing M_x and increasing M_y). The switching curves thus predict the activation pattern of the different mus-

cles in response to the above exercise. This phenomenon is referred to in this paper as the mechanical recruitment of low back muscles.

The symmetric properties of the muscle activity surfaces of contralateral pairs of muscles are reflected in their switching curves. Since the surfaces are symmetric with respect to the $M_y = 0$ plane, the switching curves and the recruitment order of the muscles on the right side of the body are going to be mirror images of the left-side muscles. Figure 7(A) illustrates this concept for the bilateral pair of iliocostalis muscles: the switching curve of the right muscle is a mirror image of the left muscle, if a mirror is placed along the M_x axis. The left muscle is activated in the counter-clockwise direction, whereas

the right muscle is activated in the clockwise direction, again, two directions that are mirror images of one another.

The redundant information in Fig. 7(A) can be eliminated by referencing the muscle to the direction of applied load. Hence, the ipsilateral muscle will be the muscle on the same side as the load, whereas the contralateral muscle will be the the muscle opposite the loading side. Figure 7(B) illustrates this idea for the iliocostalis muscle: the switching curve predicts that the muscle will always be active if the load is applied contralaterally to it. The muscle will also be active for some loads that are applied on the ipsilateral side, depending on the combination of flexion and lateral bending moments.

By plotting the switching curves of all the muscles that cross a given level in the lumbar region, predicted patterns of muscle activation can be observed. Figure 8 describes the switching curves of all the muscles included in the model. Five functional groups which have similar switching curves can be identified. The first group includes four back muscles: 1) the lattisimus, 2) the iliocostalis, 3) the longissimus, and 4) the multifidus. The second group includes the psoas and the quadratus, while the third includes the lateral portions of the external oblique and the internal oblique and the fourth includes the medial portions of the external and internal obliques. Finally, the fifth group consists of the rectus abduminus.

The identification of the loading-plane as the ultimate determinant of muscle load distribution is also useful in describing the spinal compression caused by the muscular forces. Since the optimization problem described above is solved repeatedly for the different loading combinations (represented by the grid on the loading plane), the muscular spinal compression can be described as a scalar function defined by the loading plane. Figure 9 describes that function as a three dimensional surface over the loading plane. An examination of the surface topology reveals that this surface also has (similar to the MAS) a local minimum at $M_y = 0$ (representing pure flexion loading), and a monotonic increase in the M_x direction. Hence, minimum muscular spinal compression will be obtained for symmetric loading, arising from a given flexion moment and no lateral bending moment. Equal increases of the lateral bending moment (in the right or left directions) will result in equal increases in the
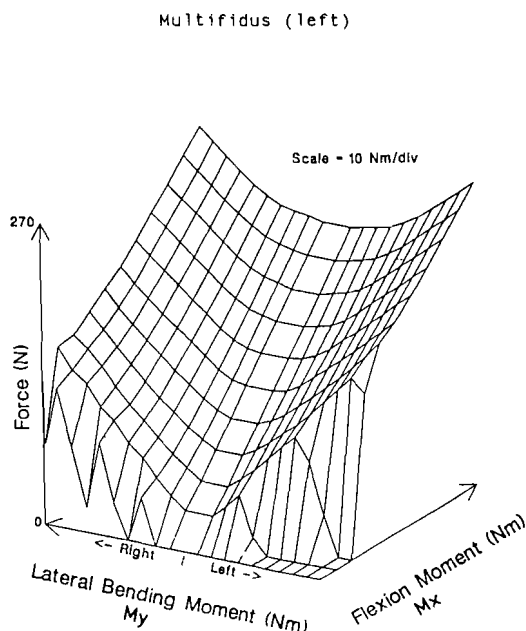
Fig. 5 Muscle activity surface of the left multifidus
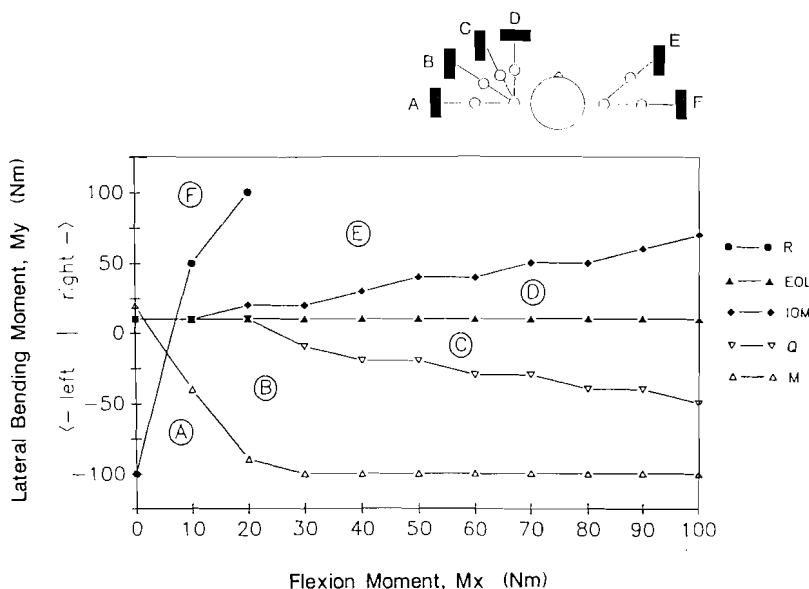

Flexion Moment, Mx (Nm)

Fig. 6 Switching curves of five muscles on the left side of the body: M-multifidus, Q-quadratus, IOM-internal oblique (medial portion), EOL-external oblique (lateral portion), R-rectus abdominus. The activation occurs in the counter-clockwise direction. A—F represent different loading conditions (given by the inset and described in the text).

value of the spinal compression force. Hence, the surface described in Fig. 9 is symmetric with respect to the plane $M_y = 0$.

Validation experiments were designed to test the model's on/off predictions. Three lumbar muscles that were accessible to surface electrodes, and were representative of the lumbar cross-section were chosen: the rectus abdominus, the medial external obliques, and the multifidus muscle of the erector spinae group. Three isometric, single-arm weight-holding tasks that were predicted by the model to activate these lumbar muscles were chosen. These three tasks were 0, 45, and 90 deg horizontal abduction of the shoulder with the elbow extended and holding a 45 N weight. Subjects performed these tasks with both the right and left arms and repeated each task once.

The external moments created by these tasks were mapped onto the loading plane as shown in Fig. 10, which also shows the switching curves for the three muscles on the left side. The points labeled A, B, and C represent the mapping of 90, 45,

and 0 deg horizontal abduction tasks of the right arm, respectively. From this figure, predictions were made as to the activity state of the muscles, and those predictions are summarized in Table 2. Similar analysis was carried out for all the six muscles in the process of performing the left arm tasks. These predictions were compared to the experimental EMG RMS traces from the muscles while subjects performed the various tasks. The right side of Fig. 10 shows the EMG tracings of the left medial external obliques for the three right arm tasks. From the switching curves, the left medial external obliques should be active only for tasks B and C. The EMG trace for task A is essentially flat, indicating the muscle did not modify its activity level. In the traces for both tasks B and C there is a noticeable activation pattern that shows an increase in the EMG signal amplitude as the subject begins the task, a relatively constant amplitude as the task is performed, and then a notable decrease in the signal amplitude when the task is completed (complete details of the experimental validation can be found in Ladin et al., 1989). From Fig. 10 and the predictions in Table 2, we see that there is perfect correlation between the model predictions and the experimental observations of the left medial oblique muscle for this subject while performing the three holding tasks. For the eight subjects tested, and the six tasks, two sets (since each task was repeated once) of 48 predictions, were made for each muscle examined. The overall success rate of our predictions was 81 and 82 percent correct predictions for the two data sets, respectively.

Discussion

The application of external loads to the upper half of the body requires the activation of muscle groups in the lumbar region to oppose those loads while maintaining a fixed body posture. A free body diagram created at an imaginary transverse cross-section through the lumbar region can be used to write the static equilibrium equations. The effect of the external loads can be lumped by determining the resultant forces and moments that are transferred to the lumbar region (a total of three force components and three moment components in the most general case). Hence, the particular details of a given
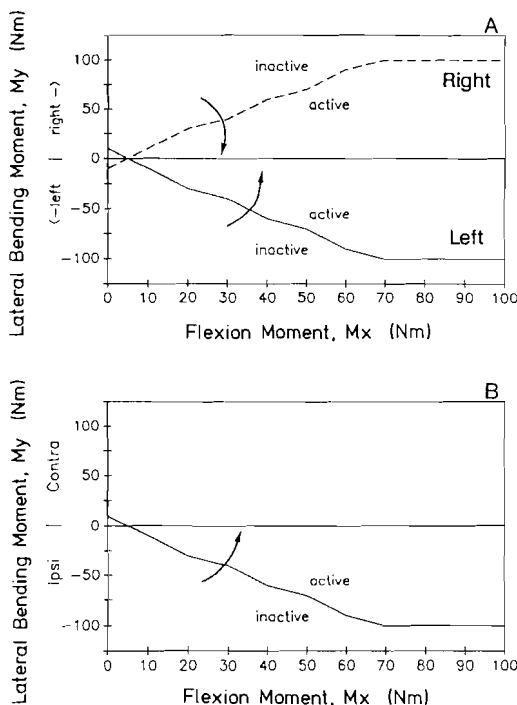
Fig. 7 Switching curves of the bilateral pair of iliocostalis muscles (A) and the equivalent switching curve of the iliocostalis muscle referenced to the direction of load application (B)

Table 2 Activation predictions for left side muscles for validation experiments

TASK	RECTUS ABDOMINUS	MEDIAL OBLIQUE	ERECTOR SPINAE
90° Horizontal Abduction	OFF	OFF	ON
45° Horizontal Abduction	OFF	ON	ON
0° Horizontal Abduction	ON	ON	ON
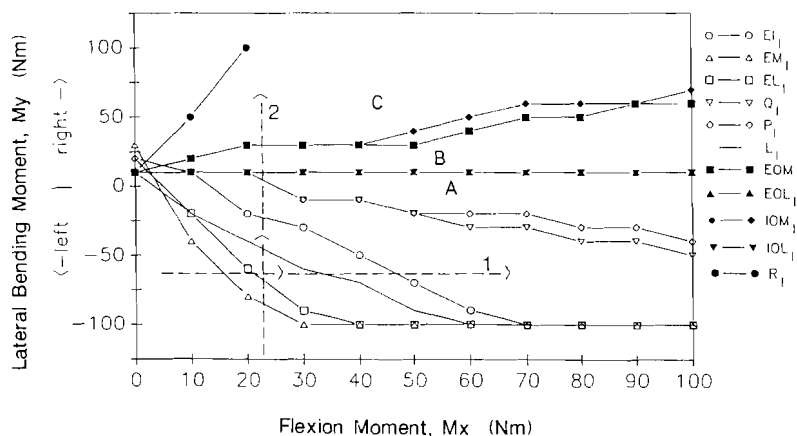
Fig. 8 Switching curves of the muscles in the lumbar region. Line 1 represents a loading exercise maintaining a constant lateral bending moment, and Line 2 represents a constant flexion bending moment.

loading condition will affect the distribution of muscle forces only if the resulting moments or forces are different.

Following the above approach it is clear that if the physical tasks are limited to gravitational loads, i.e., holding different weights in the hands, only two independent variables determine the distribution of the muscular forces in the lumbar region: the flexion moment, M_x, and the lateral bending moment, M_y. The optimization approach described in this paper proposes a cost function that is equal to the sum of the axial components of the individual muscle forces. The forces are constrained to be positive and the stresses are bounded by a maximum value. The overall spinal compression is assumed to balance the external forces, e.g., the loading weights and the muscular forces. Thus, under the above conditions, with the optimization scheme subject to gravitational loading, the actual muscle force distribution is determined for a given loading condition or (M_x, M_y) combination. The process of studying the muscle force patterns is therefore *decoupled* from the details of the physical task generating that pattern. Furthermore, since any loading combination described by (M_x, M_y) uniquely determines the indi-

vidual muscle force, an individual muscle's tension can be summarized in the form of a three-dimensional surface which spans the (M_x, M_y) plane.

The muscle force patterns shown in Figs. 1 and 2 show the effect of a 90 deg rotation in the arm holding a 50 N weight-from a pure lateral bending moment (Fig. 1) to a roughly pure flexion moment (Fig. 2). The decrease in the lateral moment and the complementary increase in the flexion moment cause a decrease in the activity of the anterior and lateral muscles on the contralateral (with respect to the weight holding arm) side with the rectus abdominus and the medial components of the external obliques completely inactivated, and an increase in the activity of the ipsilateral muscles of the equivalent erector spinae group, i.e., the iliocostalis, the longissimus, and the multifidus. This corresponds to the intuitive notion that as the flexion moment increases the back muscles need to become more activated, and that as the lateral bending moment increases, the contralateral muscles, both the abdominal and the spinal, must increase their activity levels. Such an increase in the activity of the lateral parts of the erector spinae was observed by Jonsson (1970).

The uniform stress distribution shown in Figs. 1(b) and 2(b) reflects the upper bound stress constraint that was applied to all the muscles. The numerical value of this stress level was increased until the constraint equations could be satisfied. Since only three constraint equations exist, three muscles are expected to have stress levels that are lower than the maximum, while all the rest will have the uniform upper bound stress. In situations of nearly pure lateral bending only, reducing the external load level from 50 N to 20 N reduced the stress from 216 kPa to 112 kPa in all the contralateral muscles except for the multifidus, while raising the stress levels in the ipsilateral rectus abdominus and the contralateral multifidus.

Since there are no studies to date (to the best of our knowledge) that were successful in actually measuring low back muscle forces, one can only compare the model force predictions to the published results of other models, and to studies of maximum muscle force output. In a biomechanical sagittal plane analysis of lifting, Hutton and Adams (1982) calculated the force in the erector spinae of an unloaded person in a stooped position as 2540 N and in a squat position as 1920 N. The total force in the same muscle group in our model, in response to a 50 N load held laterally in the right hand is 435 N, well within the capability of a human subject. In an elaborate model of the thoraco-lumbar spine, Yettram and Jackman (1980) calculated the muscle load distribution in forward flexion of an eleven-year old boy. According to their calculations, the iliocostalis at the L_3 level changes from 10.8 N in
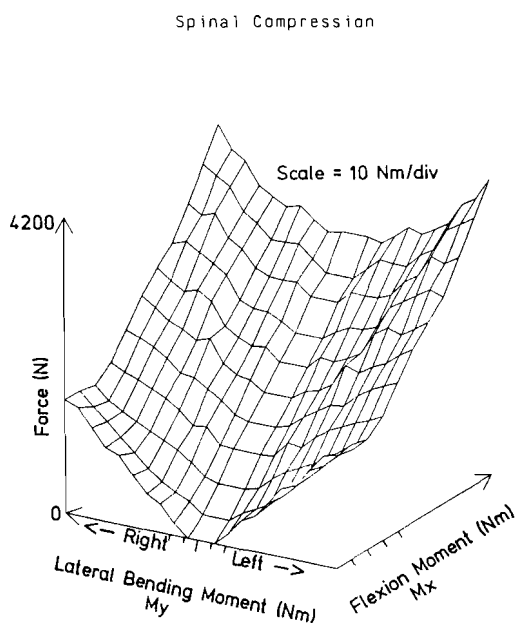

Fig. 9 Spinal compression surface; spinal compression arising from muscular activity of lumbar muscles (defined over the loading plane)
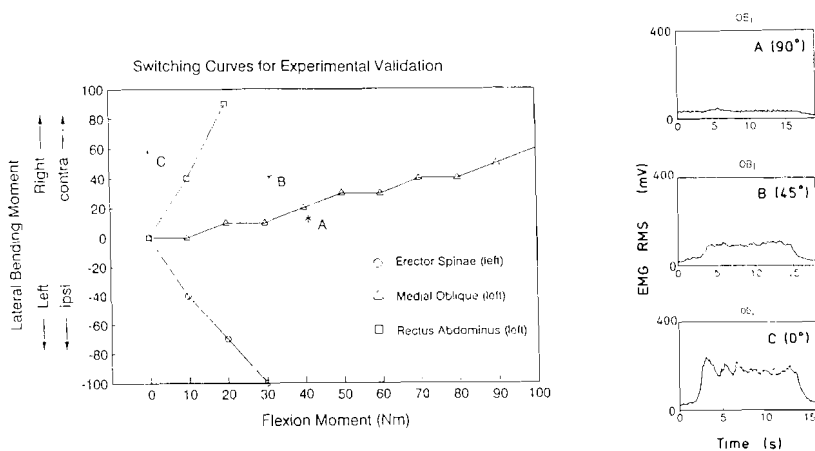

Fig. 10 Switching curves (left) for the three muscles for validation experiments. The right side of this figure displays the EMG RMS tracings for the left medial external oblique for the loading tasks A-C

the upright posture, to 206.6 N in 62 deg flexion (*with no external loading*). That analysis further predicted that the multifidus force in the same posture at the L_4 level would reach 900.9 N! Muscle stress values that correspond to such high loads will clearly exceed some estimates of the muscle stress that corresponds to maximal stimulation (150–240 kPa as reported by Powell et al., 1984), but are in line with higher estimates: 400–1000 kPa as reported by Ikai and Fukunaga (1986), and "... maximum muscular output that has been determined to be about 250 kg [2500N]" as reported by Gracovetsky et al. (1981). Our model predicted a maximum stress level of 626 kPa for a combined moment combination of a 100 Nm lateral bending moment and a 100 Nm flexion moment. This value is well within the range of maximum stress levels reported by Ikai and Fukunaga (1986).

The symmetry of the muscle activity surfaces described in Fig. 3 and detailed in Table 1 was used as a test of the internal consistency of the model: the muscle tension required to counter an external load of (M_x, M_y) is equal to muscle tension produced in the contralateral muscles in response to an external load of $(M_x; -M_y)$. Figures 3–5 show the muscle activity surfaces of the three muscles of the equivalent erector spinae group: the iliocostalis, the multifidus, and the longissimus. The surfaces share two common features: surface topology and switching curves.

The three surfaces increase with increasing the values of M_x and M_y, but all of them show a "saddle" geometry: increasing the value of M_x (for a given M_y) increases monotonically the value of the muscle tension, F. Increasing the value of M_y, on the other hand, results in a *decrease* in the muscle force until a minimum is reached at $M_y = 0$, and then a monotonic increase of F ensues. Hence, the plane $M_y = 0$ intersects the surface at the curve describing the minimum muscle tension obtained for a given M_x.

Since the plane $M_y = 0$ represents the range of symmetric bending loading (i.e., a loading condition that involves only flexion without any lateral bending), the minimum at $M_y = 0$ suggests that it is beneficial for the lumbar muscles to be loaded symmetrically whenever possible. Furthermore, since the overall spinal compression arising from muscle activity has a minimum at $M_y = 0$, the symmetric loading will minimize the load on the spine in addition to minimizing the individual muscle forces. Hence, lifting a box with *both* hands (without lateral bending) is advantageous for the spinal muscles (compared to performing the same task with one hand in a lateral lifting exercise).

The three surfaces show also a "steep rise" along the M_x direction as compared to the rise in the surface in the M_y direction (for the first nonzero points of the surface). This suggests that once a muscle is activated, it is more sensitive to changes in the flexion moment compared to the changes in the lateral bending moment. This observation is limited only to the neighborhood of the "switching curve."

The switching curve is obtained by finding the range of values (M_x, M_y) that satisfy the equation $F(M_x, M_y) = 0$. Geometrically, this curve is produced by the intersection of the muscle activity surface and the (M_x, M_y) plane. Load combinations defined by a set of values (M_x, M_y) on one side of the curve will not cause any muscular activity, as opposed to load combinations represented by points on the other side of the curve which will result in muscle activation—hence the name the 'switching curve.'

Figure 6 shows a loading exercise—moving from point A to B to C, etc.—superimposed on the switching curves of five lumbar muscles. From this figure, one can predict the recruitment order of these muscles: multifidus (M) is activated first (point B), quadratus (Q) second (point C), the lateral portion of the external obliques (EO) third (point D), and so on. This figure suggests that it may be impossible to individually activate certain muscles: since the curves intersect at approximately the

origin, any load combination that activates the quadratus will also activate the multifidus. However, these curves can be utilized (in conjuction with the actual activity surfaces) to design exercises that will use load combinations (e.g., points A-F on Fig. 6) to select a specific recruitment order and preferred muscle activity level.

The straight line labeled 1 in Fig. 8 describes a loading exercise where a fixed (negative) lateral bending moment, M_y, exists, and the flexion moment, M_x, is gradually increased. Such an exercise can be illustrated as holding a weight in the left hand and horizontally abducting the upper limb, while maintaining the load at a constant lateral distance from the body. The model predicts that the left multifidus and the longissimus muscles will be recruited first and second, respectively, followed by the latissimus dorsi and the iliocostalis. Further increases in M_x will increase the force level of these muscles without recruiting additional muscles on that side.

The above example can be contrasted with the loading exercise described by the line labeled 2. In this case the flexion moment is kept constant while the lateral bending moment is gradually increased. This can be illustrated as an exercise that moves the right hand (holding a weight) from left to right at a constant frontal distance from the body. This exercise shows a markedly different recruitment pattern as the gradual increase in loading requires the recruitment of more frontal muscles.

Increasing the flexion moment levels shows a convergence of the muscles into five functional groups of muscles in that cross section. The functional grouping suggested in this figure integrates the location, orientation and the cross-sectional areas to generate groups of muscles that are similarly activated. This may be a more appropriate way to combine different muscles into functional groups, as opposed to combining them for geometric proximity only, as suggested by Schultz et al. (1983). The grouping suggested by this paper includes the equivalent erector spinae group [iliocostalis (EI), multifidus (EM), and longissimus (EL)] and the latissimus (L) as the group to be activated first, the quadratus (Q) and the psoas (P) as the group activated second, the lateral portions of the obliques [external (EOL) and internal (IOL)] as the third, the medial portions of the obliques [external (EOM) and internal (IOM)] as the fourth and the rectus abdominus (RA) as the fifth.

The difficulty in developing a general framework to study muscle load sharing in the lower back stems from the complex anatomy and the contribution of single muscle groups to multiple moments (i.e., lateral bending, flexion, and twisting) as pointed out by Schultz et al. (1983). As a result of this difficulty, previous studies have described only limited elements of the role of lumbar muscles in opposing external loads. Serroussi and Pope (1987) presented a simple two degree-of-freedom model with which they described the effect of the external sagittal and frontal bending moments on the sum and the difference of bilateral erector spinae forces. If the EMG RMS values map monotonically with the muscle force, as stated in their assumptions, then the functional relationship between the EMG signal and the pair of values (M_s, M_f), where M_s is the sagittal bending moment (M_x in this paper) and M_f is the lateral bending moment $(-M_y$ in this paper), is identical to the muscle activity surfaces defined in this paper.

The loading plane can be used to study the role of different muscle groups in opposing external loads. Ladin et al. (1989) described a series of EMG studies that were intended to test the concept of the switching curves. Six muscles were monitored while a subject performed a set of gravitational loading exercises (i.e., holding weights in different upper limb positions, while standing erect). Using the model, predictions were made for the activity state of all the muscles (i.e., whether a muscle was predicted by the model to be active or inactive) and checked against experimental data from eight different subjects. The success rate in predicting the activity state de-

pended on the laterality of the monitored muscle with respect to the load: the muscle was referred to as ipsilateral if it was on the same side as the arm holding the weight, and contralateral if it was on the opposite side. It ranged from 100 percent (for the contralateral erector spinae-ES-in one series of trials), to 60 percent (for the ipsilateral ES). The success rate was higher for contralateral muscles (92-100 percent) than for ipsilateral muscles (60-75 percent). As the switching curves (that determine the activity state) were based on the results of the linear programming algorithm, the above results suggest that the algorithm is more successful in predicting the activity states of the contralateral muscles than of the ipsilateral muscles. The difference in the correct prediction rate may be due to the inherent property of such an algorithm to minimize cocontraction, though the classification of a muscle as "cocontracting" in cases of combined moment loading is not self-evident: a given muscle can be considered as contracting to oppose a flexion moment, yet is cocontrating when the lateral bending moment is considered. Hence, the traditional nomenclature of cocontraction should be saved to cases of pure flexion or lateral bending moments only.

One must keep in mind though, that the above predictions were based on the switching curves and the determination of the loading points on the loading plane, that were calculated for an "average male subject." Therefore, it is possible, that by accounting for the particular anatomy of each subject, one may be able to produce an individualized set of switching curves, which may improve the success rate of the model's predictions. The underlying question here relates to the sensitivity of the MASs (and the resulting switching curves) to the nature of the optimization algorithm (i.e., the cost function and the inequality constraints) and to an individual's anatomy (which would affect the equilibrium constraint equations).

A preliminary examination of the effect of the optimization approach on the switching curves was recently performed by Hughes (1989). He calculated the switching curves using the model described by Bean et al. (1988) and found them similar to the switching curves generated by this model (Ladin et al., 1989). These curves were different from those calculated for the optimization model of Hughes and Chaffin (1989). Extensive myoelectric studies of muscular activation patterns under different loading conditions, and the examination of those patterns against model predictions may identify the "correct" biomechanical model. In studying the effect of a particular anatomy on the model predictions, we have repeated the analysis for two additional anatomical cases: a large male (in the 95th percentile) and a small male (5th percentile) based on anthropometric data given by Diffrient et al. (1974). The switching curves in both cases were similar to those described for the average male in Fig. 8. They showed the same functional grouping and the same relative locations of the switching curve with respect to one another. This suggests that geometric scaling of the muscular cross-sectional areas and their location with respect to the spine will not substantially change the predicted activation patterns of the lumbar muscles.

Some suggestions of the existence of thresholds for muscle activation, e.g., switching curves, have been described in the past. Seroussi and Pope (1987) observed that activation of the external oblique muscles was dependent on a threshold value of the frontal plane moment arm. Bean et al. (1988) pointed out that shifting the load 30 deg to the right of the mid-sagittal plane will trigger the left external and internal obliques. Such an exercise is described by moving from point A to point B in Fig. 8. This figure shows the activation of the lateral portion of the internal and external obliques on the contralateral (relative to the load) side, but it also shows that the medial portions are inactive. Increasing the angle to 60 deg (point C) predicts the activation of the medial portions of the contralateral obliques, and a 90 deg rotation will activate the contralateral rectus abdominus as well. This observation was also made by

Bean et al. (1988). For pure lateral bending, the model predicts the activation of the ipsilateral rectus abdominus, but does not predict any noticeable activity of the ipsilateral obliques, as was observed by Bean et al. (1988).

The unified methodology based on the concept of the loading plane presents a convenient framework to examine previous studies of muscular activity in the lumbar region. For example, the switching curves in Fig. 8 predict that pure flexion moments ($M_y = 0$) will not cause any activity of the abdominal muscles. This result was experimentally reported by Schultz et al. (1982) in weight holding experiments. Based on a series of wire electrode measurements, Jonsson (1970) reported that a pure lateral bending moment ($M_x = 0$, $M_y > 0$) will cause no activation of the ipsilateral ES and a strong contraction of the contralateral ES. Such a result is predicted by Fig. 8: the segment of the M_y axis, which represents a lateral bending moment, lies to the left of the ipsilateral ES switching curve (thus, in the inactive region) and in the active region for the contralateral ES. He also reported that the lateral parts of the erector spinae were more active than the medial parts when pure lateral bending moments were applied. Our model predicts that for pure lateral bending ($M_y > 0$, $M_x = 0$), the multifidus, which is most medial in the ES group, contributes the smallest force. But the longissimus and iliocostalis have the same force values, even though the iliocostalis is located more laterally. Only when the external load has a flexion component in addition to the lateral bending moment did the model predict significantly larger force values in the iliocostalis.

As discussed extensively by Ladin et al. (1989), the switching curve concept was able to explain some elements of the physiological assumptions of Andersson et al. (1980), namely, that the ratio of the flexion moment to lateral bending moment determines the activity of either the ipsilateral ES or the contralateral EOM. The switching curves predict that if the flexion moment is much larger or much smaller than the lateral bending moment, only one of the two muscles is active, but there is a range of intermediate values where both muscles are predicted to be active.

Conclusion

This paper presents a new framework to study patterns of muscle activity in the lower back. The novelty of this framework lies in its identification of the loading plane as the single determinant of the lumbar muscle force distribution and its description of the muscular activity as a three-dimensional surface called a muscle activity surface, that is defined by the loading plane. This framework enabled us to examine the effect of external loading conditions on the muscle force of a given muscle, and on the load sharing among the different lumbar muscles. It is important to stress that the specific linear programming solution algorithm presented in this study serves as tool for the calculation of the MASs. As long as the underlying physiological assumption remains valid, i.e., the external moments are being equilibrated by the muscles, then one must conclude that the loading plane (or in the most general case, the loading space, which includes the torsion moment) presents a convenient form of summarizing the muscular activity for any loading condition.

The linear programming solution used in this study minimized the spinal compression force due to the muscle contraction to calculate the distribution of the muscle forces. By sequentially changing the components of the loading moments M_x and M_y, the muscle activity surface that describes the individual muscle force for a given value of (M_x, M_y) was constructed. The intersection of the MAS and the (M_x,M_y) plane creates a curve (called the switching curve) that separates the region of muscle inactivity, i.e.—the range of (M_x,M_y) values where the muscle is inactive, from the range of (M_x,M_y) values for which the muscle is active.

The examination of the switching curves describes a recruitment pattern where in response to an increase in the lateral and flexion bending moments the contralateral ES is recruited first, the psoas-quadratus group is recruited second, the lateral portion of the obliques is recruited next, followed by the medial portion of the obliques and finally by the rectus abdominus. As the recruitment order may be affected by the optimization scheme and the underlying anatomy used to generate the MAS, there is clearly a need for physiological studies and anatomical measurements to further examine the dependence of the individual switching curves on the external moments.

The examination of the individual MAS shows a monotonic increase of the force of the back muscles in response to an increase in the flexion moment, and a minimum at $M_y = 0$. (pure flexion) for an increase in the lateral bending moments. The model explains EMG recordings of muscle activity that have been described in the literature, and provides a comprehensive framework to study the role of individual muscles in responding to external loads.

Acknowledgment

References

1 Andersson, G. B. J., Ortengren, R., and Schultz, A., 1980, "Analysis And Measurement of the Loads on the Lumbar Spine During Work at a Table." *Journal of Biomechanics*, Vol. 13, pp. 513-520.

2 Bean, J. C., Chaffin, D. B., and Schultz, A. B., 1988, "Biomechanical Model Calculation of Muscle Contraction Forces: A Double Linear Programming Method," *Journal of Biomechanics*, Vol. 21, No. 1 , pp. 59-66.

3 Crowninshield, R. D., Johnston, R. C., Andrews, J. G., and Brand, R. A., 1978, "A Biomechanical Investigation of the Human Hip," *Journal of Biomechanics*, Vol. 11, pp. 77-85.

4 Crowninshield, R. D., 1978, "Use of Optimization Techniques to Predict Muscle Forces," ASME JOURNAL OF BIOMECHANICAL ENGINEERING, Vol. 100, pp. 88-92.

5 Crowninshield, R. D., and Brand, R. A., 1981, "A Physiologically Based Criterion of Muscle Force Prediction in Locomotion," *Journal of Biomechanics*, Vol. 14, No. 11, pp. 793-801.

6 Diffrient, N., Tilley, A. R., and Bardagjy, J. C., 1974, Humanscale™ 1/2/3, The MIT Press, Cambridge.

7 Eycleshymer, A. C., and Schoemaker, D. M., 1911, A Cross-Section Anatomy, Appleton Century-Crofts, New York.

8 Freivalds, A., Chaffin, D. B., Garg, A., and Lee, K. S., 1984, "A Dynamic Biomechanical Evaluation of Lifting Maximum Acceptable Loads," *Journal of Biomechanics*, Vol. 17, No. 4, pp. 251-262.

9 Golding, J. S. R., 1952, "Electromyography of the Erector Spinae in Low Back Pain," *Postgraduate Medical Journal*, Vol. 28, pp. 401-406.

10 Gracovetsky, S., Farfan, H., and Lamy, C., 1981, "The Mechanism of the Lumbar Spine," *Spine*, Vol. 6, pp. 249-262.

11 Gracovetsky, S., 1986, "Determination of Safe Load," *British Journal of Industrial Medicine*, Vol. 43, No. 2, pp. 120-33.

12 Hughes, R. E., 1989, Private communication.

13 Hughes, R. E., and Chaffin, D. B., 1989, "A New Optimization Model for Predicting Torso Muscle Force During Asymmetrical Lifting." *Proceeding of the 13th Annual Meeting of the American Society of Biomechanics*, pp. 18-19.

14 Hutton, W. C., and Adams, M. A., 1982, "Can the Lumbar Spine be Crushed in Heavy Lifting? *Spine*, Vol. 7, No. 6, pp. 586-90.

15 Ikai, M., and Fukunaga, T., 1968, "Calculation of Muscle Strength Per Unit Cross-Sectional Area of Human Muscle By Means of Ultrasonic Measurements," *Int. Z. Angew Physiol.*, Vol. 26, pp. 26-32.

16 Jonsson, B., 1970, "The Functions of Individual Muscles in the Lumbar Part of the Spinae Muscle," *Electromyography*, Vol. 1, pp. 5-21.

17 Kormodihardjo, S., and Mital, A., 1987, "Biomechanical Analysis of Manual Lifting Tasks," ASME JOURNAL OF BIOMECHANICAL ENGINEERING, Vol. 109, pp. 132-138.

18 Ladin, Z., Murthy, K. R., and De Luca, C. J., 1989, "Mechanical Recruitment Of Low Back Muscles: Theoretical Predictions and Experimental Validation," *Spine*, Vol. 14, No. (9), pp. 927-938.

19 Morris, J. M., Benner, G., and Lucas, D. B., 1962, "An Electromyographic Study of the Intrinsic Muscles of the Back in Man," *J. Anat. Lond*, Vol. 96, No. 4, pp. 509-520.

20 Patriarco, A. G., Mann, R. W., Simon, S. R., and Mansour, J. M., 1981, "An Evaluation of the Approaches of Optimization Models in the Prediction of Muscle Forces During Human Gait," *Journal of Biomechanics*, Vol. 14, No. 8, pp. 513-525.

21 Schultz, A., Andersson, G. B. J., Ortengren, R., Bjork, R., and Nordin, M., 1982, "Analysis And Quantitative Myoelectric Measurements of Loads on the Lumbar Spine When Holding Weights in Standing Posture," *Spine*, Vol. 7, No. 4, pp. 390-397.

22 Schultz, A., Haderspeck, K., Warwick, D., and Portillo, D., 1983, "Use of Lumbar Trunk Muscles In Isometric Performance of Mechanically Complex Standing Tasks," *Jounral of Orthopaedic Research*, Vol. 1, pp. 77-91.

23 Seroussi, R. E., and Pope, M. H., 1987, "The Relationship Between Trunk Muscle Electromyography and Lifting Moments in the Sagittal And Frontal Planes," *Journal of Biomechanics*, Vol. 20, pp. 135-146.

24 Yettram, A. L., and Jackman, M. J., 1980, "Equilibrium Analysis for the Forces in the Human Spinal Column and Its Musculature," *Spine*, Vol. 5, No. 5, pp. 402-11.

APPENDIX

A physical task, like weight holding, produces loading forces and torques at the $L3$ level:

$$\text{Physical task} \rightarrow \mathbf{F}_{load}, \mathbf{M}_{load}$$

From this information, static equilibrium equations at the $L3$ level that relate the individual lumbar muscle forces to the imposed external load ($\mathbf{F}_{load}, \mathbf{M}_{load}$) can be written:

$$\sum_{i=1}^{N} \mathbf{F}_i + \mathbf{F}_{load} + \mathbf{F}_{spine} = 0 \tag{1}$$

$$\sum_{i=1}^{N} \mathbf{r}_i \times \mathbf{F}_i + \mathbf{M}_{load} = 0 \tag{2}$$

where:

$\mathbf{F}_i$—individual lumbar muscle force
$\mathbf{F}_{spine}$—spinal force (force transmitted through spinal column)
$\mathbf{r}_i$—muscle centroid location with respect to vertebral body center

Since N is 22 (11 bilateral pairs) in our model, the solution of equations (1) and (2) is undetermined. Linear programming techniques are utilized to determine the muscle forces.

External Loads

The external loads consist of the loads due to the weights of various body segments and due to the weights being held in the task under investigation. These elements result in six equations (three for the forces, three for the moments) that describe the external loading effects:

$$F_X = 0 \tag{3a}$$

$$F_Y = 0 \tag{3b}$$

$$F_Z = W_t + W_h + \sum_{j=1}^{2} (W_{a_j} + W_{fa_j} + W_{l_j}) \tag{3c}$$

$$M_X = \sum_{j=1}^{P} (W_{a_j} y_{a_j} + W_{fa_j} y_{fa_j} + W_{l_j} y_{l_j}) \tag{3d}$$

$$M_Y = \sum_{j=1}^{P} (W_{a_j} x_{a_j} + W_{fa_j} x_{fa_j} + W_{l_j} x_{l_j}) \tag{3e}$$

$$M_Z = 0 \tag{3f}$$

where:

W_t—weight of the trunk
W_h—weight of the head
W_{a_j}—weight of the arm of limb j
W_{fa_j}—weight of the forearm of limb j
W_{l_j}—weight of the carried load in limb j
P—number of limbs participating in the task (either 1 or 2)
F_X, F_Y, F_Z—resultant external forces at the lumbar cross-section

M_X, M_Y, M_Z—resultant external moments at the lumbar cross-section

x^*_j, y^*_j—projections of load application points of limb j onto the lumbar cross section

The imaginary transverse cross-section is in the X, Y plane and the vertical axis is in the Z direction. Thus the external force is applied only in the vertical or Z axis which creates a flexion-extension moment M_X and a lateral bending moment M_Y on the L3 cross-section. The anthropometric data used in the above equations are based on the *Humanscale* series from M.I.T. press (Diffrient et al., 1974).

Muscle Tensile Forces

The external loading moments are balanced by the muscle tensile forces. The moment generated by a single lumbar muscle consists of the product of the muscle tensile force and the muscle moment arm (the distance from the center of the vertebral body to the centroid of the muscle). Thus the three moment equations (one for each direction X, Y, Z) become:

$$M_X = \sum_{i=1}^{N} y_i F_{Z_i} \tag{4}$$

$$M_Y = \sum_{i=1}^{N} x_i F_{Z_i} \tag{5}$$

$$M_Z = \sum_{i=1}^{N} y_i F_{X_i} + \sum_{i=1}^{N} x_i F_{Y_i} \tag{6}$$

where:

M_X, M_Y, M_Z—the external loading moments defined in equation (3) $F_{X_i}, F_{Y_i}, F_{Z_i}$—the X, Y, Z components of the individual muscle forces x_i, y_i—muscle moment arms in the X and Y direction, respectively

Expanding the M_x equation for our model yields the following equation:

$$M_X = -y_r(R_1 + R_r) - y_{eol}(\cos \delta)(EOL_1 + EOL_r)$$
$$- y_{eom}(\cos \delta \cos 30 \deg)(EOM_1 + EOM_r)$$
$$- y_{iol}(\cos \beta)(IOL_1 + IOL_r)$$
$$- y_{iom} \cos \beta \cos 30 \deg (IOM_1 + IOM_r) + y_p(P_1 + P_r)$$
$$+ y_q(Q_1 + Q_r) + y_l(\cos \gamma)(L_1 + L_r) + y_{em}) + y_{em}(EM_1 + EM_r)$$
$$+ y_{el}(EL_1 + EL_r) + y_{ei}(EI_1 + EI_r) \tag{7}$$

where:

M_X—the external flexion-extension moment
δ, β, γ—the muscle fiber angles
y_r, y_{eol}, y_{eom}, etc.—the individual muscle moment arms in the Y direction
R_l, R_r, EOM_l, EOM_r, etc.-muscle tensile forces
Note: the cos 30 deg reflects the fact that the medial obliques lie in a plane 30 deg to sagittal plane (Schultz et al., 1983)

Similarly for the moments in the Y and Z directions, the following equations are generated:

$$M_Y = x_r(R_1 - R_r) + x_{eol}(\cos \delta)(EOL_1 - EOL_r)$$
$$+ x_{eom}(\cos \delta \cos 30°)(EOM_1 - EOM_r)$$
$$+ x_{iol}(\cos \beta)(IOL_1 - IOL_r)$$
$$+ x_{iom} \cos \beta \cos 30°(IOM_1 - IOM_r) + x_p(P_1 - P_r)$$
$$+ x_q(Q_1 - Q_r) + x_l(\cos \gamma)(L_1 - L_r) + x_{em}(EM_1 - EM_r)$$
$$+ x_{el}(EL_1 - EL_r) + x_{ei}(EI_1 - EI_r) \tag{8}$$

$$M_Z = x_{eol}(\sin \delta)(EOL_r - EOL_1)$$
$$+ x_{eom}(\sin \delta \cos 30 \deg)(EOM_r$$
$$- EOM_1) + x_{iol}(\sin \beta)(IOL_1 - IOL_r)$$
$$+ x_{iom}\sin \beta \cos 30°(IOM_1 - IOM_r)$$
$$+ x_l(\sin \gamma)(L_r - L_1) \tag{9}$$

where only muscles that are not purely axial contribute to the torsion moment.

Thus equations (7)-(9) represent three equilibrium constraints for the twenty-two muscle force unknowns that arise due to the external loads.

Muscle Force Determination

As there are twenty-two unknowns and only three equations, the system is algebraically indeterminate. To calculate the unknown muscle forces, an optimization scheme using linear programming methods was employed.

The optimization scheme consists of the definition and minimization of a cost function subject to a series of equality and inequality constraints. While there are a number of cost functions that can be utilized, Schultz et al. (1983) reported that the scheme that produced the best correlations between predicted muscle forces and measured electromyographic signals used the minimization of the spinal compression while placing an upper boundary on the muscle stresses. A modified version of this scheme, which defined the cost function as the spinal compression due *ONLY* to the muscle forces, was employed in this model. Thus the following cost function was generated:

$$C_s = R_l + R_r + EOL_l \cos \delta$$
$$+ EOL_r \cos \delta + EOM_l \cos \delta \cos 30 \deg$$
$$+ EOM_r \cos \delta \cos 30° + IOL_l \cos \beta + IOL_r \cos \beta$$
$$+ IOM_l \cos \beta \cos 30° + IOM_r \cos \beta \cos 30°$$
$$+ P_l + P_r + Q_l + Q_r + L_l \cos \gamma + L_r \cos \gamma \tag{10}$$
$$+ EM_l + EM_r + EL_l + EL_r + EI_l + EI_r$$

Minimization of this cost function is constrained by the moment equations (7)-(9) above. That is, the muscle force distribution that minimizes equation (10) must also satisfy the moment equations.

In addition to utilizing the moment equations as equality constraints, the muscle stress (force/cross-sectional area) was utilized as a boundary or inequality constraint. Thus, the solution space was further bounded by the following inequality:

$$\frac{F_i}{A_i} \leq \sigma_{max} \tag{11}$$

where:

F_i = the tensile force in muscle i
A_i = the cross-sectional area of muscle i

The cross-sectional information used in this study is based on the area ratios published by Schultz et al. [1983] and on the trunk width and depth data from the *Humanscale* series.

The algorithm consisted of minimizing the cost function while satisfying the above conditions. A starting maximum stress value was selected and solution of the above equations was attempted. If no solution could be found with these boundaries, σ_{max} was incremented by a given step size until a solution was found.

The algorithm was implemented in FORTRAN using the IMSL library routine DDL-PRS (this routine is found in the IMSL library V10.0). The initial value of σ_{max} was 100 Pa and was incremented by 100 Pa until a solution was found. A number of different step sizes were used and it was found that this was the largest value of the step size that still allowed the algorithm to reach a stable solution (i.e., any step size smaller than 100 Pa yielded the same muscle force values, but increased the computational burden). Once the muscle forces were determined for a given combination of $M_X - M_Y$ plane (M_X:0-100 Nm, M_Y: $- 100$-100 Nm) was traversed. The data were then plotted as a three dimensional surface $F_i(M_X, M_Y)$, or muscle activity surface, using the RS/1 software package from Bolt, Beranek and Newman Inc..